Journal of Chemical Technology and Metallurgy, 59, 5, 2024, 1109-1118

EXPLORING THE STRUCTURAL AND ELECTRONIC CHARACTERISTICS OF AMORPHOUS Ge – Te - In MATERIAL THROUGH AB INITIO METHODS

Andi Zaidan[1,2], Vladislava Ivanova[3], Plamen Petkov[3], Pavlina Bancheva-Koleva[3]

[1]*Institute of Life Science, Technology, and Engineering*
Universitas Airlangga, 60115, Surabaya, Indonesia
[2]*Department of Physics, Faculty of Science and Technology*
Universitas Airlangga, 60115, Surabaya, Indonesia
[3]*Department of Physics, Thin Film Technology Laboratory,*
University of Chemical Technology and Metallurgy
8 Kliment Ohridski Blvd., 1797 Sofia, Bulgaria
E-mail: ivanova_vl@uctm.edu

Received 16 May 2024
Accepted 29 June 2024
DOI: 10.59957/jctm.v59.i5.2024.13

ABSTRACT

This study employs density functional theory (DFT) and molecular dynamics to meticulously investigate the structural and electronic properties of ternary chalcogenide compounds, specifically $(GeTe_4)_{1-x}In_x$*, and* $(GeTe_5)_{1-x}In_x$ *across a range of compositions (* $x = 0, 5, 10, 15, 20$ *at %). Utilizing the local density approximation within the framework of first-principles calculations, we comprehensively analyze the pair correlation function, static structural factor, electronic density of states, and electronic band gap energy. Our results reveal a notable decrease in the energy band gap of Germanium-Tellurium with the incorporation of Indium atoms. The structural changes observed in the Ge-Te matrix with Indium doping, as evidenced by the changes in the pair correlation function and static structure factor, are consistent with and supportive of the observed decrease in the band gap energy. This phenomenon is primarily attributed to the significant contribution of Indium atoms to the conduction band edge, offering new insights into the material's electronic behaviour.*

Keywords: molecular dynamics, structural properties, electronic properties chalcogenide glasses.

INTRODUCTION

Chalcogenide glasses, renowned for their distinct physical properties, have emerged as materials of significant interest in the realms of optoelectronics and electronics. Characterized by low phonon energies, impressive optical transparency in the infrared (IR) region, and a high refractive index, these materials are pivotal in a multitude of cutting-edge applications. They are integral to the development of phase-change materials [1 - 5], sensors [6 - 10], and various optical components such as circuits, gratings, and waveguides [11 - 15]. Among these, Germanium-Tellurium (Ge-Te) based chalcogenides have been the subject of extensive research, primarily due to their potential as versatile phase-change materials. This broad range of applications underscores the importance of a deeper understanding of these materials, particularly at the structural and electronic levels.

Despite the technological importance and widespread use of Ge-Te-based chalcogenides, there remains a notable gap in the theoretical framework guiding their application, especially in the context of Ge-Te-In (Germanium-Tellurium-Indium) systems. This gap is most evident in the limited understanding of their structural and atomic-scale properties. These aspects are critical for customizing materials for specific technological applications and optimizing their performance. To address this deficiency, our research focuses on a detailed theoretical analysis of the structural and electronic properties of ternary chalcogenides, particularly $(GeTe_4)_{1-x}In_x$, and $(GeTe_5)_{1-x}In_x$ across a range of compositions (x = 0, 5, 10, 15, 20 at %). This study aims to fill the existing knowledge gap and provide a comprehensive understanding of these complex materials.

In our study, we employ melt-quenching ab initio molecular dynamics simulations, an advanced technique that integrates density functional theory (DFT) with molecular dynamics (MD). This method, initially developed by Car and Parrinello, is exceptionally effective for exploring the amorphous structures of complex materials like Ge-Te-In alloys. Our research aims to uncover how Indium doping affects the structural and electronic properties of Ge-Te systems. The results of this investigation are expected to significantly contribute to the theoretical understanding of these alloys. Furthermore, our findings have the potential to lead to the development of new materials with enhanced properties for optoelectronics and electronics, promising both technological advancements and a deeper insight into material science.

EXPERIMENTAL

Generally, the simulation method used in this work corresponds to the method used in experiments and consists of two parts. First part is samples preparation. In order to obtain the amorphous Ge-Te-In material, chalcogenide $(GeTe_4)_{1-x}In_x$, and $(GeTe_5)_{1-x}In_x$ with x = 0, 5, 10, 15, 20 at % is prepared using melt quenching technique. The second part is samples characterization using DFT.

Ab initio Molecular Dynamics

Ab initio molecular dynamics fundamentally differs from classical molecular dynamics in the treatment of particle interactions. While classical molecular dynamics relies on pre-defined potentials based on empirical data to model these interactions, ab initio molecular dynamics extends beyond this traditional approach. The cornerstone of ab initio methods is the calculation of forces acting on nuclei directly from electronic structure calculations, rather than predetermined empirical potentials.

The essence of any molecular dynamic's methodology revolves around the approach to modeling interatomic interactions. Traditionally, molecular dynamics has relied on pre-determined potentials. These potentials are often complex, breaking down the full interaction into various components like two-body, three-body, and many-body contributions, along with long- and short-range terms. Each of these components requires specific functional forms for representation. After decades of intensive research, sophisticated and elaborate interaction models have been developed, encompassing the intricate aspects of these interactions.

In contrast, electronic structure-based molecular dynamics, particularly the ab initio type, offers a more dynamic approach. This method can be further categorized into two primary techniques. The first is the 'on the fly' method, where electronic structure calculations are performed concurrently with the generation of the molecular dynamic's trajectory. The second involves constructing the potential energy surface in advance, using high-dimensional fitting based on highly accurate ab initio electronic structure calculations. The diversity, breadth, and sophistication of these techniques are well-documented across various monographs, conference proceedings, and scientific literature.

The 'on the fly' approach is particularly noteworthy for not integrating out electronic variables in advance but treating them as active degrees of freedom. This allows for the handling of chemically complex systems in molecular dynamics simulations. However, it shifts the approximation from the level of selecting a model potential to choosing a specific approximation for solving the Schrödinger equation. This shift underlines the ability of ab initio molecular dynamics to explore more complex and nuanced systems than traditional molecular dynamics, marking a significant advancement in the field of molecular simulations.

Melt Quenching Technique

Currently, there is no universally accepted standard method for modeling amorphous structures using molecular dynamics (MD) techniques. While various amorphous systems have been successfully generated using the melt-quenching technique, the specifics of this method can vary considerably. Melt-quenching can be implemented using classical or ab initio MD, or a combination of both. In our research, the detailed process of the melt-quenching technique is illustrated in Fig. 1.

As depicted in Fig. 1, our melt-quenching process

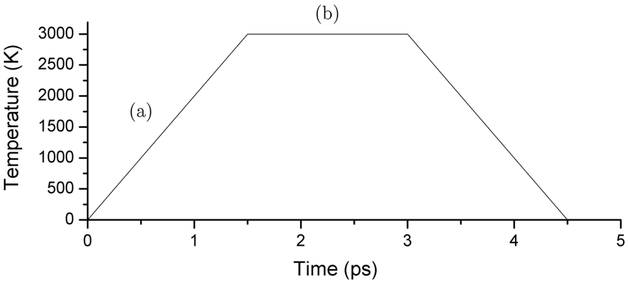

Fig. 1. Melt quenching process with (a) annealing ab initio molecular dynamics and (b) canonical ab initio molecular dynamics.

encompasses four ab initio MD steps, two annealing phases, one canonical MD, and a final relaxation step. This simulation sequence begins by sequentially conducting MD simulations, with each subsequent simulation using the structure from the previous step as its starting point. Following this, the process is reversed to cool the system back to room temperature, and then further relaxed to zero temperature. To ensure each MD simulation eliminates any correlation to its preceding structure, the system is given adequate time to reach thermal equilibrium. At each targeted temperature, the system undergoes a simulation period of 1.5 picoseconds to attain thermodynamic equilibrium. The time step for simulations is set at 3 femtoseconds for temperatures below 2500 K and is reduced to 2 femtoseconds at temperatures above 2500 K, enhancing accuracy and minimizing numerical errors at higher temperatures [16, 17]. A Nosé thermostat is employed to realize a canonical ensemble, subtly altering Newtonian MD by adding an extra degree of freedom. This allows for the fluctuation of the total energy of the system, ensuring more realistic simulation conditions.

Periodic Boundary Condition

Computer simulations inherently involve studying systems with a limited number of particles, confined within a finite cell of specific geometry. In the study of homogeneous macroscopic systems, properties are generally considered to be independent of interfaces. Therefore, accurately addressing finite size effects becomes a crucial aspect of numerical simulation methods. This approach enables the extrapolation of macroscopic quantities from simulations of relatively small systems. To emulate an infinite system, simulations often employ periodic boundary conditions. This means that a particle exiting the simulation box on one side is seamlessly reintroduced on the opposite side, creating an illusion of an unbounded environment.

In this research, all results are derived from simulations using our in-house developed Amorphous Material Modelling (A.M.M.) code. The A.M.M. code has been specifically tailored for the analysis of amorphous materials and is adept at performing the melt-quenching technique as well as analysing structural, electronic, and optical properties of these materials. A.M.M. greatly depends on other codes such as SIESTA [18, 19] and RINGS [20].

RESULTS AND DISCUSSION

Pair Correlation Function and Static Structure Factor

The positions of atoms in each sample after the relaxation process are illustrated in Fig. 2. We use a cut-off distance ranging between 2.7 and 3.3 Å to analyse the coordination number of the samples. The color-coding in Fig. 2 represents the distribution of coordination numbers: white for 0, turquoise for 1, burlywood for 2, forest green for 3, grey for 4, red for 5, brown for 6, purple for 7, and light steel blue for 8. This colour scheme aids in visualizing the distribution of various coordination states within the samples.

The pair correlation function, g(r), is a crucial tool for understanding the structure of our system. It provides detailed information about how particle densities vary as a function of distance, revealing insights into the arrangement and distribution of particles. By analysing g(r), we can determine the degree of order, identify characteristic distances between particles, and understand how the local environment influences the overall structure. This makes the pair correlation function an essential parameter in analysing and interpreting the structural properties of the system.

In amorphous materials, g(r) typically shows a prominent peak corresponding to the average atomic separation between neighbouring atoms, followed by less pronounced peaks at greater distances. This function not only sheds light on the average interatomic distances but also reveals information about defects within the material. For our Ge-Te-In system, we calculated the total and partial pair distribution functions using a 3 Å cut-off distance. Our analysis indicates that certain

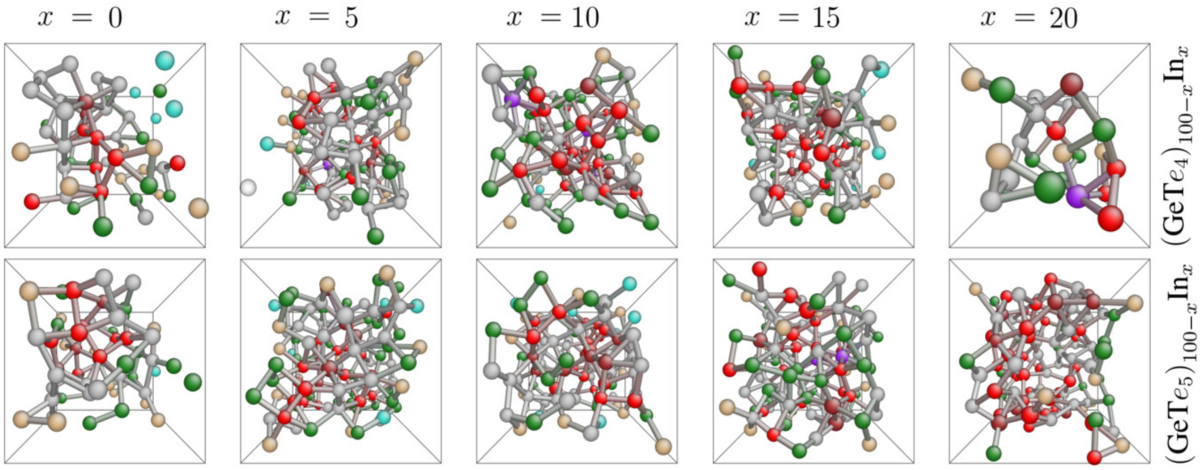

Fig. 2. Final positions of atoms for models of $(GeTe_4)_{1-x}In_x$, and $(GeTe_5)_{1-x}In_x$ with x = 0, 5, 10, 15, 20 at %. Color shows distribution of coordination number (turquoise: 1, burlywood: 2, Forest green: 3, grey: 4, red: 5, brown: 6, purple: 7).

partial pair correlations are more dominant than others. For instance, g(r) derived from X-ray data is predominantly influenced by the Te-Te pair correlation, while neutron diffraction data is more reflective of the Ge-Te pair correlation. This leads to slight discrepancies in the intensity and position of the first sharp diffraction peak (FSDP) between X-ray and neutron pair correlation functions.

By analysing partial pair distribution functions, we can precisely calculate interatomic distances. Our calculations revealed interatomic distances between Germanium and Tellurium, Germanium and Indium, and Tellurium and Indium, which vary across different compositions. For example, in the $(GeTe_4)_{95}In_5$, composition, these distances are 0.384 Å, 0.219 Å, and 0.439 Å, respectively (Fig. 3), while in the $(GeTe_4)_{90}In_{10}$, composition, they are 0.543 Å, 0.163 Å, and 0.223 Å (Fig. 3). Notably, the broadening of peaks, such as the first peak of g(r) [Te-Te] in $(GeTe_5)_{95}In_5$, (Fig. 4), may be attributed to thermal vibrations or the inherent randomness of bond lengths, suggesting the presence of defects. The pair correlation for Indium exhibits an interesting periodicity, approximately 1 Å, although these fluctuations tend to neutralize in the total pair correlation function.

Structural insights into the Ge-Te-In system can also be derived from the X-ray or neutron static structure factor. While this parameter can be directly compared with experimental data, such data is not yet available. Our calculations of the static structure factor for the Ge-Te-In system indicate that Te-Te pairs predominantly influence the peak of S(q) in both X-ray and neutron scattering, whereas Ge-Ge pairs have a minimal effect. A key point of discrepancy is the FSDP, which is a vital parameter for comparing numerical calculations with experimental results. The FSDP values for the static structure factor of the Ge-Te-In system are summarized in Table 1.

Electronic Density of States

Understanding the Electronic Density of States (EDOS) is crucial for comprehending the properties of the Ge-Te-In system, particularly in the context of its potential for electronic device fabrication. The EDOS, g(E), measures the number of available quantum energy states per unit volume within the system. A higher EDOS at a specific energy level indicates a greater number of states available for electron occupation. Conversely, an EDOS of zero implies an absence of available states at that energy level. This information is not just integral for characterizing the electronic properties of a material, but it also helps in determining its conductive, semiconductive, or insulative nature. Additionally, EDOS is instrumental in identifying the conduction band, valence band, and the energy gap of the system.

EDOS for the systems $(GeTe_4)_{1-x}In_x$, and $(GeTe_5)_{1-x}In_x$ is

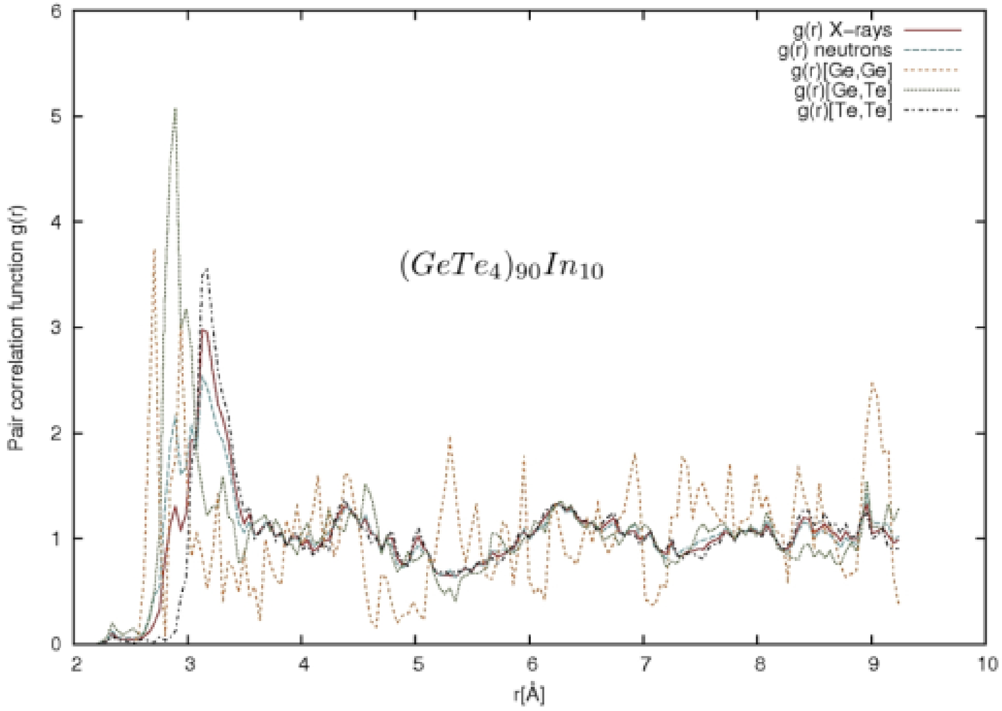

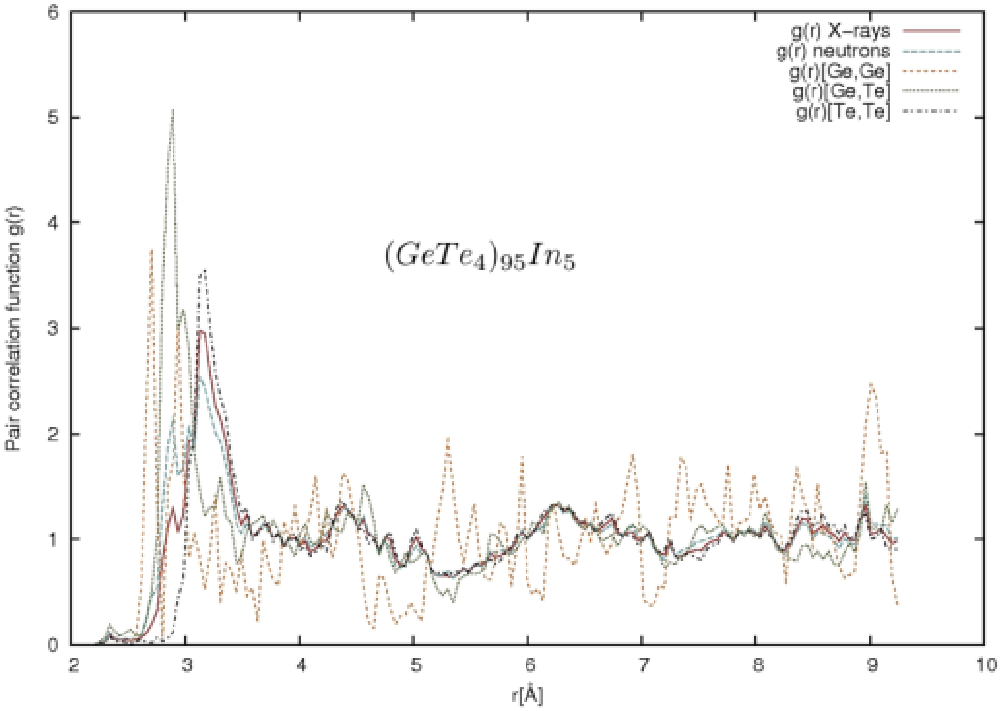

Fig. 3. Pair correlation function g(r) of selected compositions - $(GeTe_4)_{95}In_5$, and $(GeTe_4)_{90}In_{10}$, in the investigated systems.

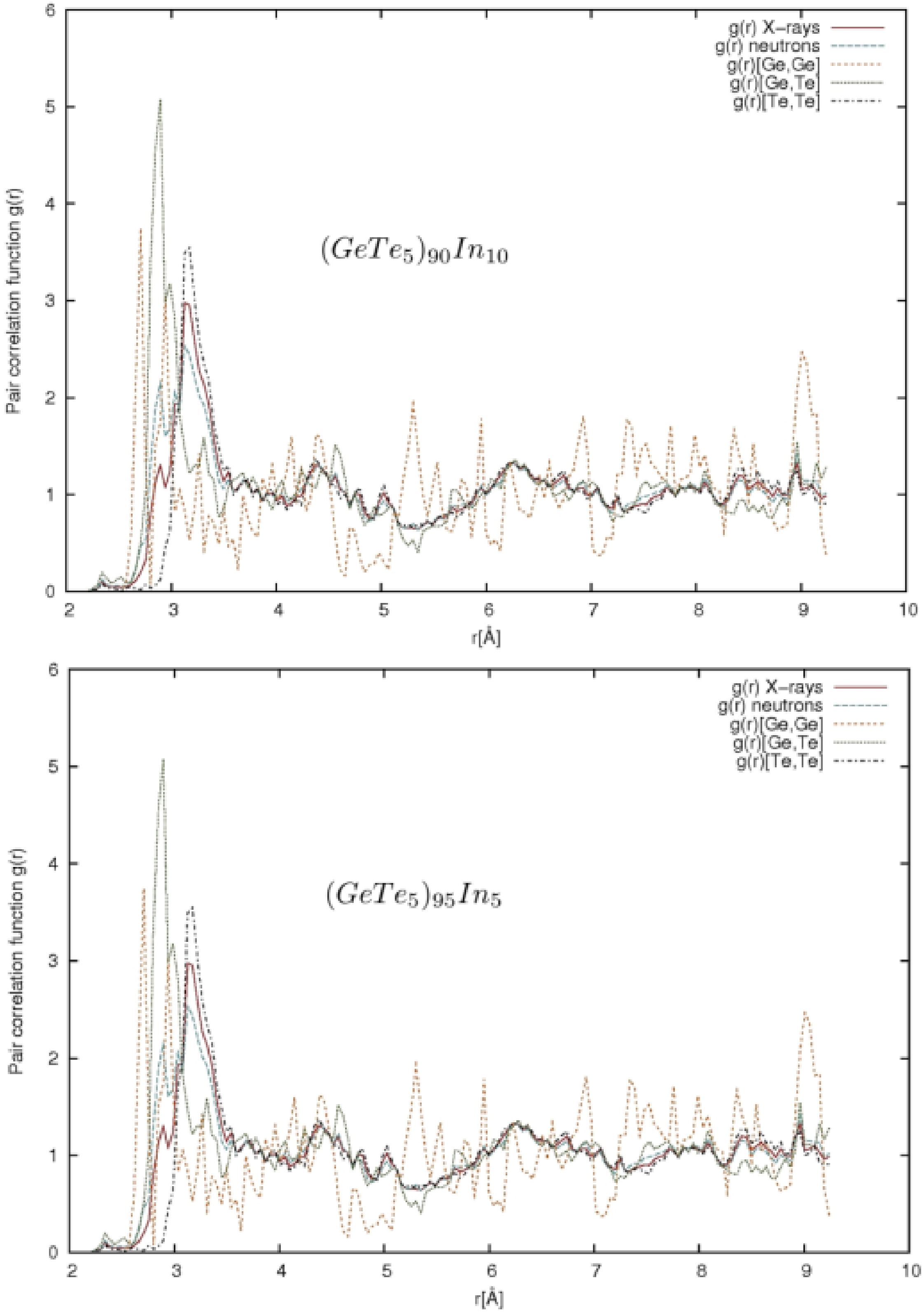

Fig. 3. Pair correlation function g(r) of selected compositions - $(GeTe_4)_{95}In_5$, and $(GeTe_4)_{90}In_{10}$, in the investigated systems.

Table 1. First and second peak of pair correlation function and static structure factor.

No	System	g(r)		S(q)	
		1st	2nd	1st	2nd
1	$GeTe_4$	2.895	3.126	2.196	4.256
2	$(GeTe_4)_{95}In_5$	2.826	3.100	2.172	4.340
3	$(GeTe_4)_{90}In_{10}$	2.849	3.120	2.229	4.295
4	$(GeTe_4)_{85}In_{15}$	2.912	3.130	2.179	4.244
5	$(GeTe_4)_{80}In_{20}$	2.858	3.063	2.110	4.156
6	$GeTe_5$	3.189	3.701	2.194	4.254
7	$(GeTe_5)_{95}In_5$	3.200	3.662	2.108	4.274
8	$(GeTe_5)_{90}In_{10}$	3.145	3.637	2.226	4.114
9	$(GeTe_4)_{85}In_{15}$	3.120	3.463	2.061	4.277
10	$(GeTe_4)_{80}In_{20}$	3.027	3.853	2.122	4.336

presented in Fig. 5 and 6. Fig. 5 reveals how the number of atoms used in the simulation influences the intensity of EDOS. In the system $(GeTe_4)_{1-x}In_x$, for instance, 25 atoms were used with x = 20, resulting in the lowest EDOS intensity. Conversely, 60 atoms for x = 0 and 100 atoms for x = 5, 10, 15 resulted in the highest intensity. It is also observed that in the Ge-Te system, the valence band edge exhibits more tailing compared to the conduction band edge. However, this trend reverses with the addition of Indium atoms, where the conduction band edge shows more tailing than the valence band edge.

Comparing the Ge-Te and Ge-Te-In systems provides insight into the electronic structure. ‘The peak observed at the conduction band in the Electronic Density of States (EDOS) is predominantly influenced by the interactions within the Ge-Te system. However, when Indium atoms are introduced, they induce a significant shift in the electronic structure. This shift is particularly noticeable at the edge of the conduction band. Specifically, Indium atoms make a substantial contribution to the conduction band in the energy range of 1.8 eV to 3.2 eV. In the conduction band, the EDOS of Indium appears to overlap with those of Germanium and Tellurium. For the $GeTe_4$ system, the results show a band gap of approximately 0.869 eV, with no states of occupation between the valence and conduction bands

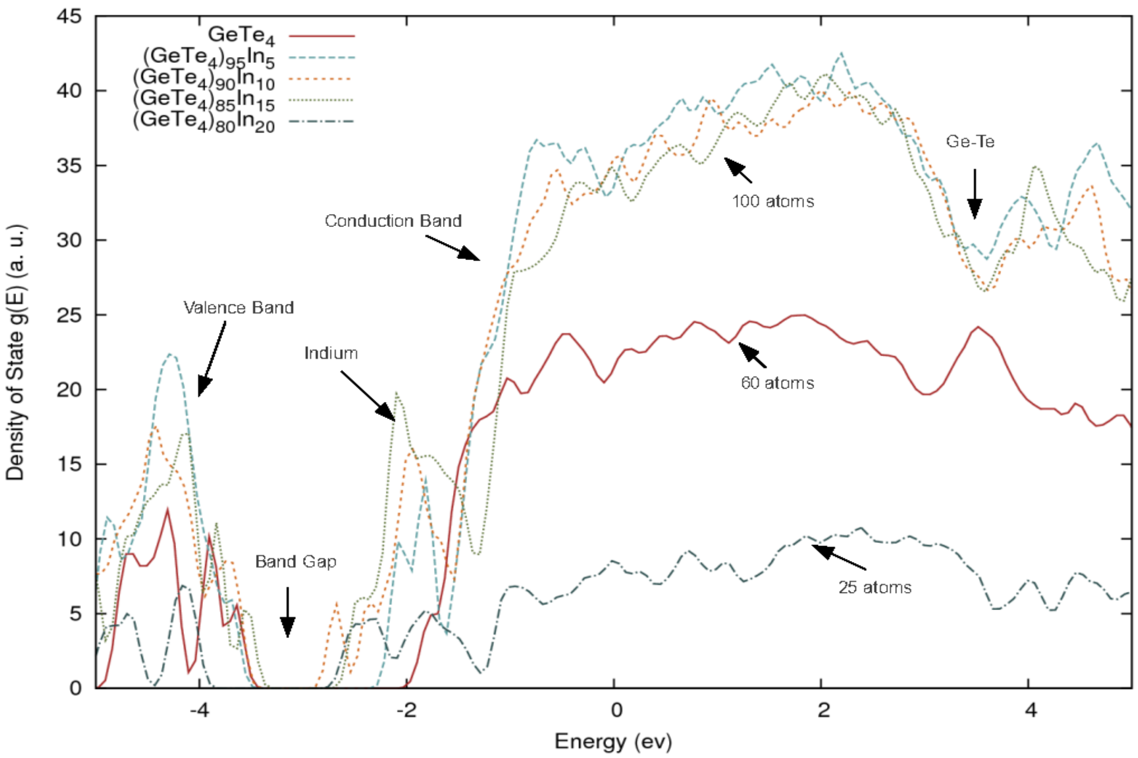

Fig. 5. Density of state of the system $(GeTe_4)_{1-x}In_x$ with x=0, 5, 10, 15, 20 at %.

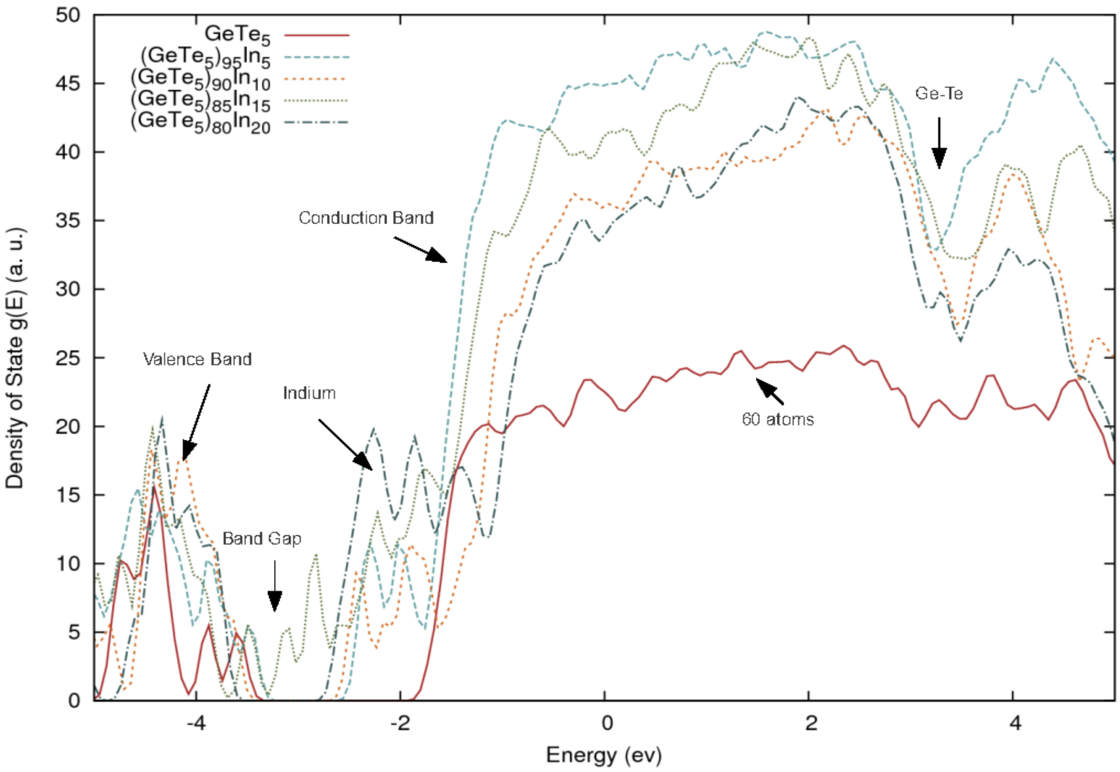

Fig. 6. Density of state of the system (GeTe$_5$)$_{1-x}$In$_x$ with x= 0, 5, 10, 15, 20.

from -3.170 eV to -2.301 eV. Similarly, in the GeTe$_5$ system, Indium's contribution to the conduction band edge is significant, with the tail of the Indium atom extending more widely, from 1.9 eV to3.2 eV.

CONCLUSIONS

In this study, we successfully simulated two ternary chalcogenide systems (GeTe$_4$)$_{1-x}$In$_x$, and (GeTe$_5$)$_{1-x}$In$_x$ with various compositions (x= 0, 5, 10, 15, 20 at %) using ab initio molecular dynamics methods. A key finding from our analysis of the partial pair distribution functions is the unique interatomic distances observed between Germanium and Tellurium, Germanium and Indium, and Tellurium and Indium in each system. These unique distances highlight the complex nature of atomic interactions within these materials and their dependence on composition.

Further, our study reveals notable characteristics in the pair correlation function, particularly in the first peak of g(r) [Te-Te]. The broadness observed in this peak for several compositions suggests the presence of defects, offering valuable insights into the structural integrity of these materials. This finding is crucial for understanding the material properties and potential applications in optoelectronics and electronics.

Additionally, the analysis of the Electronic Density of States (EDOS) has led to significant observations. The peak observed at the conduction band in the Electronic Density of States (EDOS) is predominantly influenced by the interactions within the Ge-Te system. However, when Indium atoms are introduced, they induce a significant shift in the electronic structure. This shift is particularly noticeable at the edge of the conduction band. Specifically, Indium atoms make a substantial contribution to the conduction band in the energy range of 1.8 eV to 3.2 eV. This indicates that Indium plays a crucial role in modifying the electronic properties of the system within this specific energy interval.

Acknowledgements

This study is funded by the European Union – Next Generation EU, through the National Recovery and Resilience Plan of the Republic of Bulgaria, project № BG-RRP-2.004-0002, "BiOrgaMCT".

REFERENCES

1. D. Tripathi, H.S. Vyas, S. Kumar, S.S. Panda, R. Hegde, Recent developments in Chalcogenide phase change material-based nanophotonics, Nanotechnology, 34, 2023, 502001. DOI 10.1088/1361-6528/acf1a7
2. Y. Shuang, Q. Chen, M. Kim, Y. Wang, Y. Saito, S. Hatayama, P. Fons, D. Ando, M. Kubo, Y. Sutou, $NbTe_4$ Phase-Change Material: Breaking the Phase-Change Temperature Balance in 2D Van der Waals Transition-Metal Binary Chalcogenide, Advanced Materials, 35, 2023, 2303646. https://doi.org/10.1002/adma.202303646
3. R. Golovchak, J. Plummer, A. Kovalskiy, Y. Holovchak, T. Ignatova, A. Trofe, B. Mahlovanyi, J. Cebulski, P. Krzeminski, Y. Shpotyuk, C. Boussard-Pledel, B. Bureau, Phase-change materials based on amorphous equichalcogenides, Sci Rep., 2023, 13, 2881. doi: 10.1038/s41598-023-30160-7
4. Y. Qi, N. Chen, T. Vasileiadis, D. Zahn, H. Seiler, X. Li, R. Ernstorfer, Photoinduced Ultrafast Transition of the Local Correlated Structure in Chalcogenide Phase-Change Materials, Phys. Rev. Lett., 2022, 129, 13, 135701.
5. S. Heidari, N. Nozhat, Wideband polarization-independent plasmonic switch based on GST phase-change material, Applied Optics, 2022, 61.
6. P. Kumbhakar, M.S. Sha, C.S. Tiwary, A.G.A. Muthalif, S. Al-Maadeed, K.K. Sadasivuni, An efficient transition metal chalcogenide sensor for monitoring respiratory alkalosis, Biotech., 2023, 13, 109.
7. J. Pan, Q. Li, Y. Feng, R. Zhong, Z. Fu, S. Yang, W. Sun, B. Zhang, Q. Sui, J. Chen, Y. Shen, Z. Li, Parallel interrogation of the chalcogenide-based micro-ring sensor array for photoacoustic tomography, Nature Communications, 2023, 14, 3250.
8. L. Wang, F. Xu, C. Zhang, S. Wageh, O.A. Al-Hartomy, B. Zhang, T. Yang, H. Zhang, Chemiresistive gas sensor based on Mo0.5W0.5S2 alloy nanoparticles with good selectivity and ppb-level limit of detection to ammonia, Microchimica Acta, 2023, 190, 8. DOI: 10.1007/s00604-023-05843-7
9. B. Badamchi, W.-C. Hsu, Al-A.A. Simon, Z.Y. Chi, J. Manzi, M. Mitkova, A.X. Wang, H. Subbaraman, Ultra-compact hybrid silicon: chalcogenide waveguide temperature sensor, Optics Express, 2022, 30, 16, 28470-28478. https://doi.org/10.1364/OE.462691
10. X. Zhang, C. Zhou, Y. Luo, Z. Yang, W. Zhang, L. Li, P. Xu, P. Zhang, T. Xu, High Q-factor, ultrasensitivity slot microring resonator sensor based on chalcogenide glasses, Optics Express, 2022, 30, 3, 3866-3875. https://doi.org/10.1364/OE.450092
11. Z. Wang, Z. Yang, H. Wang, W. Zhang, R. Wang, P. Xu, High-Q chalcogenide racetrack resonators based on the multimode waveguide, Appl. Opt., 2023, 62, 9, 2278-2282. doi: 10.1364/AO.484821.
12. L. Bodiou, M. Baillieul, V. Nazabal, J. Lemaitre, A. Benardais, S. Meziani, N. Lorrain, Y. Dumeige, P. Němec, J. Charrier, Carbon dioxide mid-infrared sensing based on Dy3+-doped chalcogenide waveguide photoluminescence, Optics Letters, 2023, 48, 5, 128-1131.
13. K. Xia, Z. Yang, P. Zhao, P. Yang, P. Xu, L. Xu, X. Peng, W. Zhang, S. Dai, R. Wang, Q. Nie, Supercontinuum generation in As2S3 chalcogenide waveguide pumped by all-fiber structured dual-femtosecond solitons, Opt. Express, 2023, 31, 18, 29440-29451. doi: 10.1364/OE.498193.
14. B. Shen, H. Lin, F. Merget, S.S. Azadeh, C. Li, G.-Q. Lo, K.A. Richardson, J. Hu, J. Witzens, Broadband couplers for hybrid silicon-chalcogenide glass photonic integrated circuits, Optics Express, 2019, 27, 10, 13781-13792. https://doi.org/10.1364/OE.27.013781
15. X. Zhao, H. Ma, H. Cai, Z. Wei, Y. Bi, X. Tang, T. Qin, Lead Chalcogenide Colloidal Quantum Dots for Infrared Photodetectors, Materials, 2023, 16, 17, 5790. https://doi.org/10.3390/ma16175790
16. J. Si, Y. Ma, Ab Initio Molecular Dynamics Simulations of Amorphous Metal Sulfides as Cathode Materials for Lithium-Sulfur Batteries, The Journal of Physical Chemistry C, 2023, 127, 49, 23541-23550. DOI: 10.1021/acs.jpcc.3c04835
17. B. Focassio, G.R. Schleder, F.C. de Lima, C. Lewenkopf, A. Fazzio, Amorphous Bi2Se3 structural, electronic, and topological nature from first principles, Physical Review B, 2021, 104, 21, 214206.
18. E. Artacho, E. Anglada, O. Diéguez, J.D. Gale, A. García, J. Junquera, R.M. Martin, P. Ordejón, J.M. Pruneda, D. Sánchez-Portal, J. M. Soler, The SIESTA method; developments and applicability,

J. Phys.: Condens. Matter., 2008, 20, 064208. DOI 10.1088/0953-8984/20/6/064208

19. A. García, N. Papior, A. Akhtar, E. Artacho, V. Blum, E. Bosoni, P. Brandimarte, M. Brandbyge, J.I. Cerdá, F. Corsetti, R. Cuadrado, V. Dikan, J. Ferrer, J. Gale, P. García-Fernández, V.M. García-Suárez, S. García, G. Huhs, S. Illera, R. Korytár, P. Koval, I. Lebedeva, L. Lin, P. López-Tarifa, S.G. Mayo, S. Mohr, P. Ordejón, A. Postnikov, Y. Pouillon, M. Pruneda, R. Robles, D. Sánchez-Portal, J.M. Soler, R. Ullah, V. W. Yu, J. Junquera, Siesta: Recent developments and applications, J. Chem. Phys., 2020, 152. 204108. https://doi.org/10.1063/5.0005077
20. S. Le Roux, P. Jund, Ring statistics analysis of topological networks: new approach and application to amorphous GeS2 and SiO2 systems, Computational Materials Science, 2010, 49, 1, 70-83. https://doi.org/10.1016/j.commatsci.2010.04.023